WORLD CONFERENCE ON TIMBER ENGINEERING 2025
BRISBANE, AUSTRALIA
Advancing Timber for the Future Built Environment

THE EFFECT OF DISPLACEMENT RATE ON THE AXIAL LOAD CAPACITY OF STEEL RODS GLUED INTO GLULAM BEAMS

Knight L.[1], Toumpanaki E.[2]

ABSTRACT: Glued-in rod (GiR) timber connections are being increasingly used for structural connections due to their high stiffness, axial load transmission, and connection efficiency. Studies have been conducted on various factors impacting the performance of glued-in rods, such as glue-line thickness, moisture content, and rates of loading for small loading rates. The impact of higher rates of loading is less known and is critical for understanding the connection performance under accidental loading scenarios. This study investigated the relationship between the rate of loading (ROL) and the axial withdrawal capacity of steel threaded rods (M12) bonded into softwood glulam (GL24) with a structural two-part adhesive (glue-line thickness of 2 mm). The specimens were tested in a 'pull-pull' configuration under four rates of loading: 1, 10, 100, and 1000 mm/min, with the latter ROL representing accidental loading. The axial withdrawal load capacity and stiffness at the serviceability and ultimate limit state were found to increase with an increase in ROL. The stiffness was found to be more sensitive to loading rates, as determined by a one-way ANOVA analysis. The design equations for the axial withdrawal load capacity and stiffness at the serviceability from the new draft version of Eurocode 5 did not agree well with the experimental findings. Rate of loading modification factors were proposed to account for instantaneous loading scenarios.

KEYWORDS: Timber connections, Glued-in rods, Rates of loading, Axial withdrawal strength, Axial withdrawal stiffness.

1 – INTRODUCTION

Glued-in Rods (GiRs) provide an effective method for establishing a high-performance connection without the need of oversizing structural timber elements, thus avoiding the overall expensive solutions often associated with dowel connections. GiRs are being used increasingly in retrofitting over other methods, such as metal shear plates or exposed bolts, as they offer more lightweight and aesthetically pleasing solutions. Although a general-purpose design procedure within Eurocode 5 will be provided in the second generation of Eurocodes [1], there has been much debate in design equations for the axial withdrawal performance of GiRs. Part of this debate is relevant to the impacts of accidental loading. A new Informative Annex A on *Additional guidance for increasing the robustness of timber structures* is included in [1]. This new Annex includes direct design methods with specific scenarios that account for the effects of local failure and dynamic load factors, as well as overstrength factors, which are provisionally prescribed [2]. The only UK guidelines, BS EN 17334:2021 [3], cover test standards for GiRs and basic design principles in Annex A. National Annexes to Eurocode 5, such as DIN EN 1995-1-1/NA [4], and the New Zealand Timber Design Guide [5] provide design guidance for GiRs using different design equations.

Despite significant research on the axial withdrawal capacity of GiRs under tensile monotonic loading and low rates of loading (as typically employed in timber test standards), there is limited understanding of their performance under accidental loading and high rates of loading (ROLs). Recommended overstrength factors in Annex A in [1] rely on the ratio of the 95th-percentile to the 5th-percentile load carrying capacity value of a connection without considering dynamic effects. Overstrength factors for GiRs, which account for accidental loading and are supported by experimental results, become increasingly important when designing timber buildings to resist disproportionate collapse, particularly for tall timber structures that require high-performance connections and also to withstand the increased tying loads from the catenary action.

1.1 GLUED-IN RODS

Glued-in rods are a type of connection in which a rod (metal, composite, timber, etc.) is bonded into a hole made in another material, such as timber, using adhesives like

[1] Louis Knight, Structural Engineer, Prime Engineering, lknight@primeengineering.fr.

[2] Eleni Toumapnaki, Civil, School of Aerospace and Design Engineering (CADE), Bristol Composites Institute group, University of Bristol, Bristol, United Kingdom, email: eleni.toumpanaki@bristol.ac.uk, ORCID: https://orcid.org/0000-0002-4208-3284

https://doi.org/10.52202/080513-0169

epoxies or polyurethanes. There are many variables that can impact the capacity of GiR connections, such as the adhesive (type and thickness), type of rod, and the type of wood being glued into (including grain direction) [6]. Variations in specific curing conditions, including the temperature and moisture of the wood during adhesive application, also exist between types and manufacturers of adhesives [7]. The construction of GiR connections on site can pose several challenges, including centering the rod in the hole, addressing air pockets within the adhesive, ensuring a consistent depth of the rod, and maintaining a suitable installation speed. Voids are the most critical manufacturing defect in GiRs, resulting in a decrease of approximately 25% in the axial withdrawal capacity [8]. However, off-site installation of GiRs offers high-quality control, and once complete, the assembly of structural timber members on-site is easy and quick. The most common material for rods is steel due to its material properties, which allow for a ductile connection design. Standard threaded rods perform well due to the increased surface area for adhesion between the rod and the glue [9]. Other alternatives which have been explored are fibre-reinforced polymer (FRP) rods [10-11], reinforcement bars [12], and wooden dowels.

Extensive research has been carried out to assess key parameters that affect the axial withdrawal performance of GiRs (e.g., timber density, bonded length, rod diameter, etc.), whereas more recent studies have focused on lateral load capacity [13-14]. Some studies have addressed the insertion angle of the GiR with respect to the grain direction, which affects failure modes and axial withdrawal performance due to timber's anisotropic properties. Loading parallel to the grain direction most frequently produces failures at the wood/resin interface where the shear strength of the wood is weaker than the rod/resin interface [15]. Loading perpendicular to the grain direction results in timber rolling shear failures and pull-out strengths 20-50% higher compared to GiRs loaded parallel to the grain [16]. GiRs perpendicular to the grain direction engage a larger area of wood at failure, which possibly contributes to the higher failure loads. Timber density was found to have a more significant impact on the failure load when GiRs were loaded perpendicular to the grain direction as opposed to parallel [16].

A current knowledge gap exists in the performance of GiRs under accidental loading and high rates of loading (ROLs). Timber and adhesives, as viscoelastic materials, are more sensitive to strain-rate effects than threaded steel rods. At high ROLs, both steel and timber show improved mechanical performance, and steel's ductile performance declines. The relationship between the enhanced mechanical performance of these interconnected materials and the reduction in ductility influences the overstrength factors, which can change when considering high ROLs in timber structures. Moreover, connection stiffness can increase at high ROLs, and a significantly stiffer connection in timber frames can restrict rotational capacity, resulting in brittle timber failure modes in the vicinity of the joint. Therefore, it is important to understand how the axial withdrawal performance and failure modes in GiRs are affected by high ROLs.

1.2 Effect of Rate of Loading

Timber

It is well-documented that the strength properties of timber are higher when subjected to higher ROLs due to its viscoelastic nature and microstructural changes. Green et al. [17] reported a 20% increase in the mechanical properties of wood with a ten-fold increase in strain rate, showing an exponential relationship between strength and loading rate across several orders of magnitude loading. A 10% increase in load required to induce failure in a wooden sample in 1 s has been reported in [18] as opposed to a static test (failure in 5 min). The highest rate of loading effect has been noted in specimens tested under tension perpendicular to the grain. Furthermore, high ROLs significantly influence performance at higher moisture levels (wet compared to dry wood), particularly during bending [19].

Steel

Steel has also a well-documented trend of an increase in ultimate tensile strength due to an increase in ROL. Cadoni and Forni [20] reported that the steel proof and ultimate tensile strengths increased by around 10-20% with a rate increase from 250 to 950 strain/s for steel plate samples. These findings are in agreement with Qin et al. [21] and Sun et al. [22]. Importantly, the latter found a similar trend whereby further increases in strain rates (from 1750 to 2650 strain/s) resulted in negligible changes to the capacity of TRIP800 steel. Li and Chen [23] observed a much higher increase (up to 75%) in ultimate tensile strength capacity for steel grades Q355, Q460, and Q620 when the strain rate was increased to 3000/s compared to the quasi-static case. It should be noted that the 'Q' designation refers to the first letter of the Chinese word for the yield strength of steel. These steels are essentially equivalent to the European equivalent standard 'S' graded steels, with the number following the letter dictating the yield strength of the steel. As the strain rate increases, the strain-hardening rate, which is responsible for the increased strength, decreases [24]. Stress-strain curves from tensile testing

of steel sheets at intermediate strain rates (1/s to 200/s) showed that low-strength steel is more strain-rate sensitive than high-strength steel, and the strain-rate sensitivity is a strong function of strain for the strain-hardening term. The most common model to predict steel's behaviour as a function of the strain, strain rate, and temperature is the Johnson-Cook model [25] (Equation 1). This model follows the trend of greater capacities for higher strain rates, similar to Airing's molecular activation model for epoxy-based adhesives.

$$\bar{\sigma}=[A+B\bar{\varepsilon}^{n}]\left[1+C\ln\left(\frac{\dot{\bar{\varepsilon}}}{\dot{\varepsilon_0}}\right)\right]\left[1-\left(\frac{T-T_{room}}{T_{melt}-T_{room}}\right)^{m}\right] \quad (1)$$

where $\bar{\sigma}$, $\bar{\varepsilon}$, $\dot{\bar{\varepsilon}}$, $\dot{\varepsilon_0}$, T_{room}, and T_{melt} are flow stress, plastic strain, effective strain rate, reference strain rate (1 s^{-1}), room temperature, and melting temperature, respectively. A, B, C, n, and m are all constants.

Adhesives and Adhesive joints

Similarly to timber, adhesive has a well-documented increase in strength when loaded to failure over a shorter period. The importance of designing a connection while considering higher loading rate scenarios, particularly with adhesives, was emphasised by Yildiz et al. [26] when it was found that the energy absorption of aluminium-epoxy and steel-epoxy joints decreased dramatically when an increase in ROL was considered. Similar findings were reported by Khalil and Bayoumi [27] and Wade and Cantwell [28]. Both projects found a decrease in energy absorption of adhesive joints, emphasising the importance of analysing the behaviour of adhesive under faster loading rates. Similar ROLs, up to 1000 mm/min, as in the current study, were adopted in [28]. Quasi-static loading gives the joint more time to absorb energy compared with fast loading scenarios and accidental loading. It should be noted that although there has been a decrease in fracture toughness, this doesn't imply a reduction in the ultimate tensile strength with an increase in ROL. In fact, Banea et al. [29] found that the ultimate tensile strength of high-temperature epoxy adhesives increased logarithmically with an increase in ROL. The study used dog-bone shaped specimens and covered values of ROL from 0.1 mm/min to 10 mm/min, which is significantly lower than the rates found during accidental loading situations. However, the approximately 10% increase in ultimate tensile strength at 10 mm/min found in 29] is significant for such low range of ROL. This is consistent with the Airing's molecular activation model [29], described by Equation 2.

$$\sigma=A_1\left[1+A_2\left(\frac{T}{T_g}\right)\log\left(\frac{\gamma}{\gamma_0}\right)\right] \quad (2)$$

where σ is the ultimate tensile stress (MPa), T is the temperature (°C) and γ is the test speed (mm/min). A_1, A_2, and γ_0 are material constants.

No effect of ROL in the failure modes of epoxy-bonded cylindrical butt joints was found in [30]. Similar to other studies, a decrease in energy absorption was recorded at high strain rates, with brittle adhesives exhibiting little strain-rate dependency. An increase in ultimate strength at high ROL was observed, irrespective of the adhesive type (ductile *vs.* brittle).

For GiRs, the only study that can be found in the literature regarding the effect of ROL is by Madhoushi and Ansell [31], who studied Glass Fibre-Reinforced Polymer (GFRP) rods glued in Laminated Veneer Lumber (LVL) with epoxy adhesives. Thinner glue-line thicknesses (0.5mm) in GiRs resulted in a slight increase in pull-out load capacity, whereas the inverse trend was observed for thicker glue-line thicknesses (4mm). However, considerable scatter was observed in the data, which inhibited the drawing of firmer conclusions, including trends in failure modes.

This study aims to investigate the effect of ROL on the axial withdrawal strength and stiffness of GiRs with threaded steel rods. GiR specimens were tested at four loading rates of 1, 10, 100, and 1000 mm/min to represent quasi-static and accidental loading scenarios, which can occur in the event of sudden collapse due to sudden loss of a column . Analytical equations between the axial withdrawal load capacity and stiffness at both the serviceability and ultimate limit state are established as a function of the ROL.

2 – EXPERIMENTAL PROGRAMME

2.1 MATERIALS & SPECIMEN PREPARATION

Glulam beams of grade GL24 with a final size of Depth x Width x Length = 100 mm x 100 mm x 500 mm were used to manufacture the 'pull-pull' specimens and evaluate the axial withdrawal resistance of GiRs under different rates of loading. Threaded steel rods with a nominal diameter of 12 mm (M12) and of steel grade 8.8 were used. Hence, they had a characteristic yield strength $f_{y,k}$ = 640 N/mm^2, tensile strength $f_{u,k}$ = 800 N/mm^2 , and nominal stress area $A_{s,nom}$ = 84.3 mm^2 [32]. The adhesive used was a 2-component thixotropic epoxy adhesive (Rotafix Timberset Adhesive), especially suited to bonding metal to timber.

https://doi.org/10.52202/080513-0169

A 2 mm glue-line thickness, resulting in a hole diameter of 16 mm, and a bonded length, L_b, of 140 mm were adopted. An anchorage length of 170 mm (1.2 times greater than the bonded length) and the same M12 threaded rod were used at the other end of the 'pull-pull' specimen to restrict failure on one side. The holes were cleaned of wood fiber residues with compressed air. To align the steel threaded rods while casting the epoxy, acrylic rings were placed at each end of the bonded length. The adhesive infill into the main hole was horizontally via lateral holes.

(a) (b)

Figure 1. (a) 'Pull-pull' test set up, and (b) slip measurements with LVDTs.

2.2 TEST PROCEDURE

To assess the axial withdrawal capacity of GiRs, the 'pull-pull' test method was adopted with an Instron 1342 (100 kN) machine using V-grips to accommodate the threaded rods. Figure 1(a) depicts the 'pull-pull' test set up. Two LVDTs were attached to the live end of the specimen, as shown in Figure 1(b), with their probe tips located in the same central lamination of the glulam specimen. Four nominal ROLs of 1, 10, 100, and 1000 mm/min were selected. The ROLs were later checked for inertia effects and were consistent with the nominal values. A slight difference was recorded in the highest ROL, where specimens were loaded at an average of 975 mm/min (±17 mm/min), which is 25 mm/min lower than the nominal value. This difference at that scale is small, as discussed in section 3. The data acquisition from the LVDTs recorded 1000 datapoints per second to accurately capture slippage and, consequently, axial withdrawal stiffness at the highest ROL. There was a total of 16 tests tested, 4 specimens for each ROL. The specimen nomenclature adopted is A-B-C, where A=P designates the pull-pull test, B represents the ROL (0001, 0010, 0100, or 1000), and C stands for the specimen number.

The bond shear strength, f_{vr}, was calculated by averaging the ultimate failure load over the rod surface area based on Equation 3.

$$f_{vr} = \frac{F_{max}}{d \cdot \pi \cdot l_a} \tag{3}$$

where f_{vr} is the bond shear strength (MPa), F_{max} is the maximum withdrawal failure load (kN), d is the nominal rod diameter (mm), and l_a is the nominal bonded length of steel rod (mm).

The axial stiffness at serviceability, K_{SLS}, was calculated as the gradient between 10 and 40% of F_{max} for each load-slip graph, in accordance with the definition for K_{ser} in EC5. Slip values were corrected for the elastic extension of the rod between the end grain face and the LVDT mounting system. The ultimate stiffness, K_{ULS}, for each sample was taken as the gradient of the secant between the 10% and maximum withdrawal failure load, F_{max}.

3 – EXPERIMENTAL RESULTS

3.1 SUMMARY

The axial withdrawal failure load, F_{max}, the bond shear strength, f_{vr}, the stiffness at the serviceability and ultimate limit state, K_{SLS} and K_{ULS}, and the number of pull-out (PO) failures per ROL are summarised in Table 1. It should be noted that one specimen from groups P-0001, P-0010, and P-0100 failed in the anchorage zone and was thus disregarded in the calculation of the average and standard deviation values reported in Table 1. The highest axial withdrawal capacity is recorded at the highest ROL, 10000 mm/min. This is 25% higher than the average F_{max} of the reference group at a rate of loading of 1 mm/min. A significantly higher increase in stiffness is recorded at both the serviceability and ultimate limit states at 1000 mm/min compared with the 1 mm/min reference group. A higher standard deviation is observed

https://doi.org/10.52202/080513-0169

in both the axial withdrawal capacity and stiffness at a ROL of 10 and 100 mm/min.

Table 1: Summary of experimental data.

Specimen name	ROL (mm/min)	F_{max} (kN)	f_{vr} (N/mm^2)	K_{SLS} (kN/mm)	K_{ULS} (kN/mm)	No of PO
P-0001	1	45.30 (4.19)	7.36 (0.68)	110.08 (20.74)	72.46 (19.84)	3
P-0010	10	52.08 (14.90)	8.46 (2.42)	104.31 (37.49)	75.64 (21.74)	2
P-0100	100	49.73 (13.12)	8.08 (2.60)	168.94 (52.22)	99.51 (52.35)	4
P-1000	1000	56.71 (6.82)	9.23 (1.07)	328.86 (62.87)	190.24 (30.12)	1

Note: 1) average (standard deviation), 2) PO=pull-out withdrawal failures.

3.2 FAILURE MODES

In most specimens, a pull-out failure was observed either as wood/resin interface (Figure 2a) or as a mixed mode of wood/resin interface and wood plug failure (Figure 2b). Most splitting failures (Figure 2c) were observed at the highest rate of loading (1000 mm/min), and one splitting failure was recorded at a rate of loading 10 mm/min. The glulam beams from which the specimens were derived had signs of shrinkage cracks at the ends. However, it is expected that shrinkage cracks do not affect failure loads, as reported in [11]. Moreover, no correlation was observed between shrinkage and splitting cracks. It can be inferred that a greater tendency for splitting failures occurs when GiRs are loaded at high rates, and further testing is required to enhance the structural reliability of the results. In some specimens, a denser growth ring arrangement (Figure 2d) was observed in the central lamination where the GiR was located. However, a higher axial withdrawal strength was not recorded despite the anticipated greater density.

4 – ANALYTICAL MODELLING

4.1 STATISTICAL SIGNIFICANCE

To test the statistical significance of the trends resulting from the change in the ROL, an ANOVA *F*-test analysis was conducted. The one-way analysis presented in Table 2 shows the results for all ROLs, as well as a comparison between the static case (1 mm/min) and the highest ROL (1000 mm/min). A significance level of 0.05 was chosen; therefore, a high level of statistical significance is indicated by a *P*-value of less than 0.05.

Table 2: ANOVA statistical analysis.

Variable	ROL samples	*F*	*F-crit*	*P*-value
F_{max}	All	0.637	3.863	0.6097
	1 vs 1000 mm/min	6.889	6.608	0.0468
K_{SLS}	All	27.583	3.49	<0.0001
	1 vs 1000 mm/min	43.681	5.987	0.0006
K_{ULS}	All	12.023	3.490	0.0006
	1 vs 1000 mm/min	26.553	5.987	0.0021

A very high P-value of 0.6097 showed that there is no significant difference in the average maximum pull out load (F_{max}) between different ROLs. However, when comparing only the static case to the highest ROL case the results were found to be statistically signficant, with P=0.0468. Repeating the one-way analysis on the connection stiffness parameters clearer trends were identified. For the stiffness at the serviceability limit state (K_{SLS}) there was a significant difference between the different ROLs, when comparing the extreme cases as well as all ROLs together (P-value <0.0001). The stiffness at the ultimate limit state (K_{ULS}) also resulted in high statistical significance, with a P-value of 0.0006, when comparing all ROLs. Overall, a much higher statistical significance was found in the stiffness values of the GiRs than in the axial withdrawal load capacity for all ROLs. However, it should be noted that a much higher

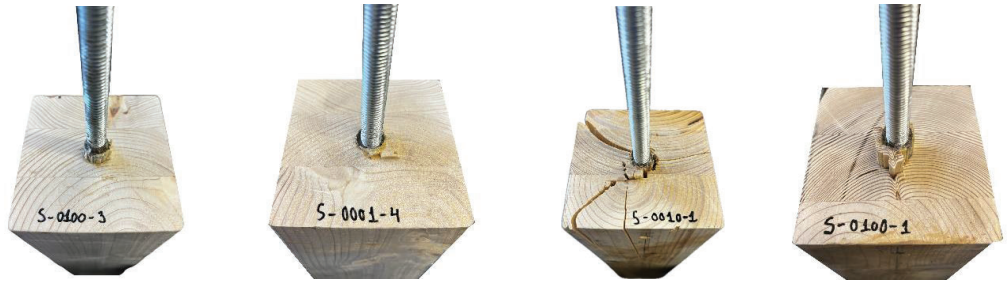

(a) (b) (c) (d)

Figure 2. Typical failure modes: (a) wood/resin interface failure, (b) mixed mode failure, (c) splitting failure, and (d) central lamination with denser growth rings.

https://doi.org/10.52202/080513-0169

scatter was observed in the experimental F_{max} values compared to the K_{SLS} and K_{ULS} values.

4.2 Modification factors for Rate of Loading (ROL)

For better clarity, the axial withdrawal capacity, F_{max}, was plotted against the corresponding ROL for each sample on a logarithmic scale (see Figure 3a). The same approach is adopted for K_{SLS} and K_{ULS}, as shown in Figures 3b and 3c, respectively. To predict the axial withdrawal performance and stiffness of GiRs in glulam timber considering higher rates of loading, analytical equations are proposed based on Equations (4) and (5), and a linear regression analysis is conducted. A similar equation was proposed in [33] for the axial withdrawal capacity of self-tapping screws in Cross Laminated Timber.

$$\frac{F_{max}}{F_{max,ref,mean}} = 1\text{-}n_{ROL,F}(1\text{-ROL}) \quad (4)$$

$$\frac{K_i}{K_{i,ref,mean}} = 1\text{-}n_{ROL,Ki}(1\text{-ROL}) \quad (5)$$

where $F_{max,ref,mean}$ = average withdrawal load capacity at a reference displacement rate (i.e., 1 mm/min), $n_{ROL,F}$ = coefficient derived from linear regression analysis by plotting the normalised load values *vs* rate of loading (ROL), K_i = axial withdrawal stiffness where i = *SLS* for stiffness at the serviceability and *ULS* for stiffness at the ultimate limit state, $K_{i,ref,mean}$ = average withdrawal stiffness at a reference displacement rate (i.e., 1 mm/min) and $n_{ROL,Ki}$ = coefficient derived from linear regression analysis by plotting the normalised stiffness values K_i *vs* rate of loading (ROL).

Table 3 summarises the n_{ROL} coefficients and the respective R^2 values derived from a least squares regression analysis on the normalized experimental data.

Table 3: Data from the least squares regression analysis.

	n_{ROL}	R^2
F_{max}	0.00026	0.0535
K_{SLS}	0.00200	0.8144
K_{ULS}	0.00160	0.7543

The analytically predicted values, derived from the n_{ROL} values and Equations (4) and (5) for the relevant axial withdrawal load capacity and stiffness, are depicted in Figure 3 for ease of comparison. A better fit between experimental and analytical data is observed for the axial withdrawal stiffness values, K_{SLS}, which agrees with the highest R^2 value reported in Table 3. Due to the high scatter in the experimental data, a low R^2 value is derived for the $n_{ROL,F}$ and Equation 4. More experimental data is required to shed light on the relationship between F_{max} and ROL and the $n_{ROL,F}$ value.

The draft version of the second generation of Eurocode 5 [1] proposes Equations 6 and 7 for the axial withdrawal capacity and stiffness of a bonded-in rod (glued-in rod).

$$F_{ax,pred} = \pi d L_b f_{vr,k} \quad (6)$$

$$K_{SLS,pred} = 2d^{0.6} L_b^{0.6} \rho_{mean}^{0.9} \quad (7)$$

where $F_{ax,pred}$ and $K_{SLS,pred}$ are the withdrawal load capacity due to shear failure (as experimentally observed here) and the axial slip modulus according to [1], respectively, d is the diameter of the rod, L_b is the bonded

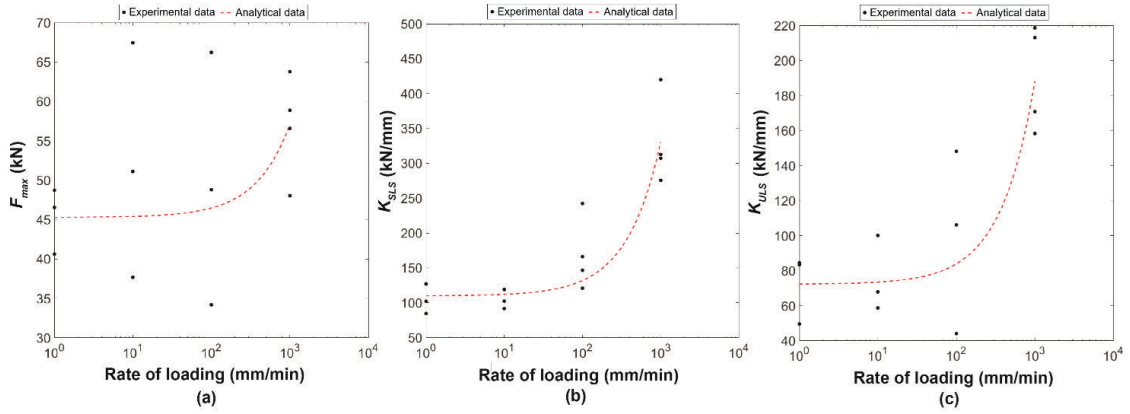

Figure 3: (a) axial withdrawal failure load, (b) stiffness at the serviceability stage and (c) stiffness at the ultimate stage with respect to the rate of loading at a logarithmic scale.

https://doi.org/10.52202/080513-0169

length, $f_{vr,k}$ is the characteristic bond shear strength (=4 MPa [1]), and ρ_{mean} is the mean density of the wood (420 kg/m^3).

Table 4 compares the predicted values according to [1] with the current experimental data. For the predicted stiffness at the ultimate limit state, the relationship $K_{ULS,pred}$ = 2/3 $K_{SLS,pred}$, as recommended in [1], was considered. To account for the increased ROLs, the modification factors, 1-$n_{ROL,F}$(1-ROL) and 1-$n_{ROL,i}$(1-ROL) were considered based on Equations 4 and 5 for the $F_{ax,pred}$ and $K_{SLS,pred}$ respectively. It should be noted that modification factors for instantaneous loading are not recommended for stiffness values in Eurocode 5.

Table 4: Comparison of predicted and experimental values.

ROL (*mm/min*)	F_{max} (*kN*)		K_{SLS} (*kN/mm*)		K_{ULS} (*kN/mm*)	
	Pred	**Exp**	**Pred**	**Exp**	**Pred**	**Exp**
1	21.1	45.3	39.6	110.0	26.4	72.5
10	21.2	52.08	40.3	104.3	26.8	75.6
100	21.6	49.73	47.4	168.9	30.6	99.5
1000	26.6	56.71	118.7	328.9	68.6	190.2

For the reference rate of loading of 1 mm/min, it can be observed that the design equations proposed in [1] significantly underestimate the experimentally observed values. The predicted axial withdrawal load capacity and stiffness (ULS and SLS) values are 53% and 64% less than the experimental ones. Similar values of K_{SLS} of glued-in steel rods in glulam and CLT have been reported in [34] and [35]. The predicted values at the highest rate of loading (1000 mm/min) are similarly much lower than the experimental ones due to the low predicted reference values (1 mm/min), irrespective of the magnitude of the modification factors that account for the ROL. Moreover, the ratio K_{ULS}/K_{SLS} in terms of experimental values ranges from 66% to 58% from 1 mm/min to 1000 mm/min. Therefore, the recommended ratio of 2/3 in [1] to calculate the K_{ULS} with respect to K_{SLS} agrees well with the current experimental findings at low rates of loading. A slightly lower ratio is recorded at 1000 mm/min.

A comparison of the analytically calculated modification factors, 1-n_{ROL}(1-ROL), at the highest rate of loading, (1000 mm/min) with the recommended k_{mod} value in [1] is made in Table 5. Instantaneous loading and a service class 1 are assumed for the k_{mod}. The k_{mod} value recommended in the second generation of Eurocode 5 [1] is much lower than the stiffness modification factor analytically calculated in this study. This can have a significant impact when designing timber structures for disproportionate collapse resistance, particularly in cases where catenary action is assumed, which requires sufficient rotational capacity. Yet, for the catenary action, an in-depth investigation of the effect of ROL on the energy dissipation capacity of GiRs is required. The k_{mod} agrees better with the analytically predicted modification factor for the axial withdrawal load capacity. Yet, considerable scatter was observed in this data. Design equations for the axial withdrawal performance of GiRs need to be revised, and rate of loading modification factors for the connection stiffness should be considered.

Table 5: Analytical modification factors at 1000 mm/min.

1-$n_{ROL,F}$(1-ROL)	1.26
1-$n_{ROL,KSLS}$(1-ROL)	3.00
1-$n_{ROL,KULS}$(1-ROL)	2.60
k_{mod} [1]	1.10

5 – CONCLUSIONS

The axial withdrawal performance of Glued-in Rods (GiRs) in glulam was assessed at four rates of loading 1, 10, 100, and 1000 mm/min, and loading rate modification factors were proposed as analytically dervided with a least-sqaures regression analysis. Key conclusions, subject to the number of specimens studied here, are summarised below:

1. An increase in the axial withdrawal load capacity and stiffness of GiRs was experimentally observed. A significantly higher increase in stiffness values was recorded compared to the failure loads.

2. A greater tendency to splitting failure modes was reported at the highest rate of rate of loading of 1000 mm/min.

3. The axial withdrawal stiffness was shown to be more sensitive to loading rates according to a one-way ANOVA analysis.

4. The design equations for the axial withdrawal load capacity and stiffness of glued-in rods in the second generation of Eurocode 5 did not agree well with the experimental findings.

5. The analytically derived rate of loading modification factors for the axial withdrawal stiffness are much higher

https://doi.org/10.52202/080513-0169

than the k_{mod} value in Eurocode 5 for an instantaneous loading scenario.

6 – REFERENCES

[1] CEN 2024. Eurocode 5 draft. Informal enquiry: prEN 1995-1-1: Design of timber structures - Part 1-1: General and rules for buildings (CEN/TC 250/SC 5 N 1488). Brussels, Belgium, 2021.

[2] P. Palma, J. Munch-Andersen and P. Dietsch. "Updating Eurocode 5 – Design guidance for increasing the robustness of timber structures." In: World Conference on Timber Engineering (WCTE 2023). Oslo, Norway, 2023.

[3] BSI. EN 17334. Glued-in rods in glued structural timber products. Testing, requirements and bond shear strength classification, British Standards Institute, London, United Kingdom, 2021.

[4] DIN (Deutsches Institut fur Normung). German National Annex to EC5. DIN EN1995-1-1/NA: 2010-12, 2010.

[5] NZTDS (New Zealand Timber Design Society). Timber Design Guide. Wellington, New Zealand, 2007.

[6] R. Steiger, E. Serrano, M. Stepinac, V. Rajcic, C. O'Neill, D. McPolin, and R. Widmann. "Strengthening of timber structures with glued-in rods." In: Construction and Building Materials 97 (2015), pp. 90-105.

[7] W. Dong, X. Gu, J. Han, and L. You. "Universal Adhesives- Different Curing Methods and Applications." In: E3S Web of Conferences, 290 (2021), 01021.

[8] N. Ratsch, S. Böhm, M. Voß, M. Kaufmann, and T. Vallée et al. (2019). "Influence of Imperfections on the Load Capacity and Stiffness of Glued-In Rod Connections." In: Construction and Building Materials. 226 (2019), pp. 200-211.

[9] G. Tlustochowicz, E. Serrano and R. Steiger. "State-of-the-art review on timber connections with glued-in steel rods." In: Materials and Structures 44 (2011), pp. 997-1020.

[10] E. Toumpanaki, and M.H. Ramage. "Glued-in CFRP and GFRP rods in block laminated timber subjected to monotonic and cyclic loading." In: Composite Structures 272 (2021), 114201.

[11] E. Toumpanaki, and M.H. Ramage. "Cyclic Loading of Glued-In FRP Rods in Timber: Experimental and Analytical Study." In: Journal of Composites for Construction (2021), 04021075-1.

[12] J. Kangas. "Timber structures with connections based on in V-Form glued-in rods." In: Finnish Civil Engineering 3 (1995), pp. 51-55.

[13] D. Fawcett, E. Toumpanaki. "Combined effects of axial and lateral loading for Glued-In steel rods in laminated veneer lumber." In: Structures 57 (2023), 105310.

[14] K. Simon, and S. Aicher. "Reinforced Rigid Glulam Jonts with Glued-in Rods subjected to Axial and Lateral Force Action." In: Proceedings of the 55th INTER (International Network on Timber Engineering) Meeting. Bad Aibling, Germany, 2022.

[15] V. Gardelle, and P. Morlier. "Geometric parameters which affect the short term resistance of an axially loaded glued-in rod." In: Materials and Structures, 40 (2007), pp. 127-138.

[16] R. Steiger, E. Gehri, and R. Widmann. "Pull-out strength of axially loaded steel rods bonded in glulam perpendicular to the grain." In: Materials and Structures 40 (2007), pp. 827-838.

[17] D.W. Green, J.E. Winandy and D.E. Kretschmann. "Mechanical properties of wood." General technical report – GTR-113 – Forest Products Laboratory, 1999.

[18] R. Ross. "Wood handbook : wood as an engineering material." General technical report – FPL-GTR-282 – , Forest Products Laboratory, 2021.

[19] C.C. Gerhards. "Effect of moisture-content and temperature on the mechanical properties of wood - An analysis of immediate effects. " In: Wood and Fiber 14 (1982), pp. 4-36.

[20] E. Cadoni, and D. Forni. "Strain-rate effects on S690QL high strength steel under tensile loading. " In: Journal of Constructional Steel Research, 175 (2020).

[21] J. Qin, R. Chen, X. Wen, Y. Lin, M. Liang and F. Lu. 2013. "Mechanical behaviour of dual-phase high-strength steel under high strain rate tensile loading. " In: Materials Science and Engineering: A 586 (2013), pp. 62-70.

[22] X. Sun, A. Soulami, K.S. Choi, O. Guzman and W. Chen. "Effects of sample geometry and loading rate on tensile ductility of TRIP800 steel." In: Materials Science and Engineering A 541 (2012), pp. 1-7.

[23] W. Li, and H. Chen. "Tensile performance of normal and high-strength structural steels at high strain rates." In: Thin-Walled Structures 184 (2023), 110457.

[24] H. Huh, J. H. Lim, and S.H. Park. "High speed tensile test of steel sheets for the stress-strain curve at the intermediate strain rate." In: International Journal of Automotive Technology 10 (2009), pp. 195-204.

[25] H.S. Nam, J.S. Kim, J.J. Han, J.W. Kim and Y.J. Kim "Ductile fracture simulation for A106 Gr.B carbon steel under high strain rate loading condition." In: Recent Advances in Structural Integrity Analysis - Proceedings of the International Congress (APCF/SIF-2014) – (2014) Oxford: Woodhead Publishing, 2014.

[26] S. Yildiz, Y. Andreopoulos, and F. Delale. "Mode I characterization of toughened epoxy adhesive joints under shock-wave loading." In: International Journal of Adhesion and Adhesives 90 (2019), pp. 71-87.

[27] A. A. Khalil, and M. R. Bayoumi. "Effect of loading rate on fracture toughness of bonded joints." In: International Journal of Adhesion and Adhesives 11 (1991), pp. 25-29.

[28] G. A. Wade and W. J. Cantwell. "Temperature and loading rate effects on the fracture behaviour of adhesively bonded GFRP Nylon-6,6" In: Journal of Adhesion 76.3 (2001), pp. 245-264.

[29] M. D. Banea, F.S.M. de Sousa, L.F.M. da Silva, R.D.S.G. Campilho, A.M. Bastos de Pereira. "Effects of Temperature and Loading Rate on the Mechanical Properties of a High Temperature Epoxy Adhesive." In: Journal of Adhesion Science and Technology 25 (2011), pp. 2461-2474.

[30] S. Murakami, Y. Sekiguchi, C. Cato, E. Yokoi and T. Furusawa. "Strength of cylindrical butt joints bonded with epoxy adhesives under combined static or high-rate loading." In: International Journal of Adhesion and Adhesives 67 (2016), pp. 86-93.

[31] M. Madhoushi and M.P. Ansell. "Experimental study of static and fatigue strengths of pultruded GFRP rods bonded into LVL and glulam. " In: International Journal of Adhesion and Adhesives 24.4 (2004), pp. 319-325.

[32] BSI: EN ISO 898-1. Mechanical properties of fasteners made of carbon steel and alloy steel. Bolts, screws and studs with specified property classes. Coarse thread and fine pitch thread. British Standards Institute, London, United Kingdom, 2013.

[33] E. Toumpanaki, A. Gawne, R. Humphreys, and L. Vojnovic. "Effect of moisture and rate of loading in the withdrawal capacity of screws in Cross Laminated Timber" In: Structures 69 (2024), 107530.

[34] J. Ogrizovic, R. Jockwer, and A. Frangi. "Seismic response of connections with glued-in steel rods." In: 6th meeting of the International Network on Timber Engineering 51-07-5, 2018.

[35] B. Azinovic, E. Serrano, M. Kramar, and T. Pazlar. "Experimental investigation of the axial strength of glued-in rods in cross laminated timber." In: Materials and Structures 51(2018), 143.

https://doi.org/10.52202/080513-0169